Geomorphology 304 (2018) 64–73

Contents lists available at ScienceDirect

Geomorphology

journal homepage: www.elsevier.com/locate/geomorph

Implications of sea-level rise in a modern carbonate ramp setting

Stephen W. Lokier [a,*], Wesley M. Court [a], Takumi Onuma [b], Andreas Paul [a]

[a] Geosciences Department, Khalifa University of Science and Technology, Petroleum Institute, P.O. Box 2533, Abu Dhabi, United Arab Emirates
[b] Applied Geoscience Department, JGI, Inc., Tokyo, Japan

ARTICLE INFO

Article history:
Received 10 April 2017
Received in revised form 13 December 2017
Accepted 16 December 2017
Available online 28 December 2017

Keywords:
Sea level
Transgression
Carbonate ramp
Coastal erosion
Persian Gulf

ABSTRACT

This study addresses a gap in our understanding of the effects of sea-level rise on the sedimentary systems and morphological development of recent and ancient carbonate ramp settings. Many ancient carbonate sequences are interpreted as having been deposited in carbonate ramp settings. These settings are poorly-represented in the Recent. The study documents the present-day transgressive flooding of the Abu Dhabi coastline at the southern shoreline of the Arabian/Persian Gulf, a carbonate ramp depositional system that is widely employed as a Recent analogue for numerous ancient carbonate systems. Fourteen years of field-based observations are integrated with historical and recent high-resolution satellite imagery in order to document and assess the onset of flooding. Predicted rates of transgression (*i.e.* landward movement of the shoreline) of 2.5 m yr^{-1} ($\pm$0.2 m yr^{-1}) based on global sea-level rise alone were far exceeded by the flooding rate calculated from the back-stepping of coastal features (10–29 m yr^{-1}). This discrepancy results from the dynamic nature of the flooding with increased water depth exposing the coastline to increased erosion and, thereby, enhancing back-stepping. A non-accretionary transgressive shoreline trajectory results from relatively rapid sea-level rise coupled with a low-angle ramp geometry and a paucity of sediments. The flooding is represented by the landward migration of facies belts, a range of erosive features and the onset of bioturbation. Employing Intergovernmental Panel on Climate Change (Church et al., 2013) predictions for 21st century sea-level rise, and allowing for the post-flooding lag time that is typical for the start-up of carbonate factories, it is calculated that the coastline will continue to retrograde for the foreseeable future. Total passive flooding (without considering feedback in the modification of the shoreline) by the year 2100 is calculated to likely be between 340 and 571 m with a flooding rate of 3.40–8.64 m yr^{-1}. However, adopting the observation that global sea-level rise only accounts for 15% of the recorded shoreline retreat, this figure rises dramatically to a total likely dynamic flooding (considering modifications to the shoreline) of between 2.3 and 3.8 km. Loss of microbial and mangal habitats will subject the exposed shoreline to increasing erosion. Shoreline retreat will threaten existing coastal infrastructure.

© 2017 Elsevier B.V. All rights reserved.

1. Introduction

The past two centuries have witnessed a rise in global sea-level at an accelerating rate, with 3.2 mm yr^{-1} observed from instrumental records over the past two decades (Church and White, 2011; Meyssignac and Cazenave, 2012; Church et al., 2013). This industrial-era signature of global sea-level rise has been documented in a range of coastal systems (Singh, 1997; Leatherman et al., 2000; Rankey and Morgan, 2002; Woodroffe, 2008; Ford and Kench, 2015; Romine et al., 2016; Testut et al., 2016). However, to date, there have not been any studies of the effects of this transgression on sedimentary systems and shoreline morphology in a carbonate ramp setting. The coastline of Abu Dhabi, lying at the southern shore of the Persian/Arabian Gulf, hereafter referred to as the Gulf, is an ideal setting for studying the process of transgression in such a setting. The overall progradational geometry for the Abu Dhabi coastline during the Late Holocene regression and stillstand is well-documented (Evans et al., 1969; Kinsman and Park, 1976; Lokier and Steuber, 2008; Stewart et al., 2011; Lokier et al., 2015). Yet only a small number of previous studies have conjectured the effects of a eustatic sea-level rise, with the creation of new accommodation that only recently overwhelmed sediment production and thus initiated the onset of a transgressive phase (Evans and Kirkham, 2002; Lokier et al., 2015).

The primary objective of this study is to utilise fourteen years of field-based observations along with historical and recent satellite imagery to document and assess the process of transgression in an arid carbonate and evaporite coastal depositional system that is morphologically analogous to numerous ancient carbonate ramp systems. The study also aims to establish the diagnostic sedimentary features that can be employed to assist in the identification of transgressive surfaces in ancient sedimentary sequences throughout the stratigraphic record. These outcomes provide a resource with which to interpret the sequence stratigraphic context in ancient carbonate ramp settings and, conversely, to

* Corresponding author.
E-mail addresses: slokier@pi.ac.ae (S.W. Lokier), onuma@jgi.co.jp (T. Onuma).

https://doi.org/10.1016/j.geomorph.2017.12.023
0169-555X/© 2017 Elsevier B.V. All rights reserved.

consider the likely implications of global sea-level rise on future shoreline morphodynamics. Furthermore, predictions of probable rates of geomorphic change are fundamental to planning future coastline management (Pethick, 2001; Romine et al., 2016).

2. Setting

The Gulf is a shallow (average 35 m) microtidal (1–2 m) epeiric sea lying at the northern margin of the Arabian Plate (Fig. 1). The floor of the almost completely land-locked basin dips gently north-eastward towards the coast of Iran. The sediments of the seafloor are dominated by muddy to fine-grained carbonates (Evans, 1966; Uchupi et al., 1996) and associated hardgrounds (Shinn, 1969). There is a general increase in siliciclastic content towards the Iranian shoreline (Emery, 1956).

The Abu Dhabi coastline of the Gulf comprises a northward-dipping, low-angle, carbonate ramp characterised by the transition from a supratidal sabkha, through a broad carbonate-dominated intertidal environment, into a subtidal carbonate setting (Evans et al., 1964). The coast is locally isolated from open-marine conditions by a complex of peninsulas, shoals and islands that formed as Holocene sediments accreted around Pleistocene limestone associated with the underlying Great Pearl Bank (Purser and Evans, 1973; Harris, 1994). The southern Gulf shoreline has been tectonically stable throughout the late Quaternary (Stevens et al., 2014).

The emirate of Abu Dhabi experiences an arid climate with a mean annual rainfall of 72 mm, concentrated during February and March as localised, brief, torrential rainstorms (Raafat, 2007). Mean annual evaporation of 2.75 m exceeds rainfall by almost 4000% (Bottomley, 1996). Temperatures measured in the study area regularly exceed 50 °C on summer days yet may drop as low as 7 °C during winter nights (Lokier and Fiorini, 2016). The prevailing wind is the northwesterly Shamal. Storms are rare and typically of relatively short duration and low energy.

3. Methods

This study utilised and integrated multiple datasets including satellite imagery, shoreline transect surveys and long-term repeat field observations along a 16 km section of coastline containing a range of settings representative of the Gulf coastal system of the UAE (Fig. 1). The study employed Quickbird data with a spatial resolution of 0.6 m/pixel for the Panchromatic Band, acquired in 2003, 2004, 2005 and 2007, and WorldView-2 data with a 0.5 m/pixel resolution for the same band acquired in 2010. Multi-band data covering the visible-near infrared region with a spatial resolution of 2.4 m/pixels and 2.0 m/pixel, for Quickbird and WorldView-2 respectively, were also used along with PAN-sharpened colour images with 0.6 m/pixel for Quickbird and 0.5 m/pixel for WorldView-2 data. Multi-band data were converted to space reflectance using parameters provided by the Technical Note of Digital Globe, and Normalized Vegetation Index images were produced in order to trace the distribution change of onshore vegetation as well as microbial mats in the intertidal zone. The resultant images were examined and compared in order to trace temporal morphological changes along the coastline.

Field-based observations have been regularly made in the Abu Dhabi sabkha since the year 2000. Though not initially focused on this specific study, the earlier field observations (prior to 2007) provided an

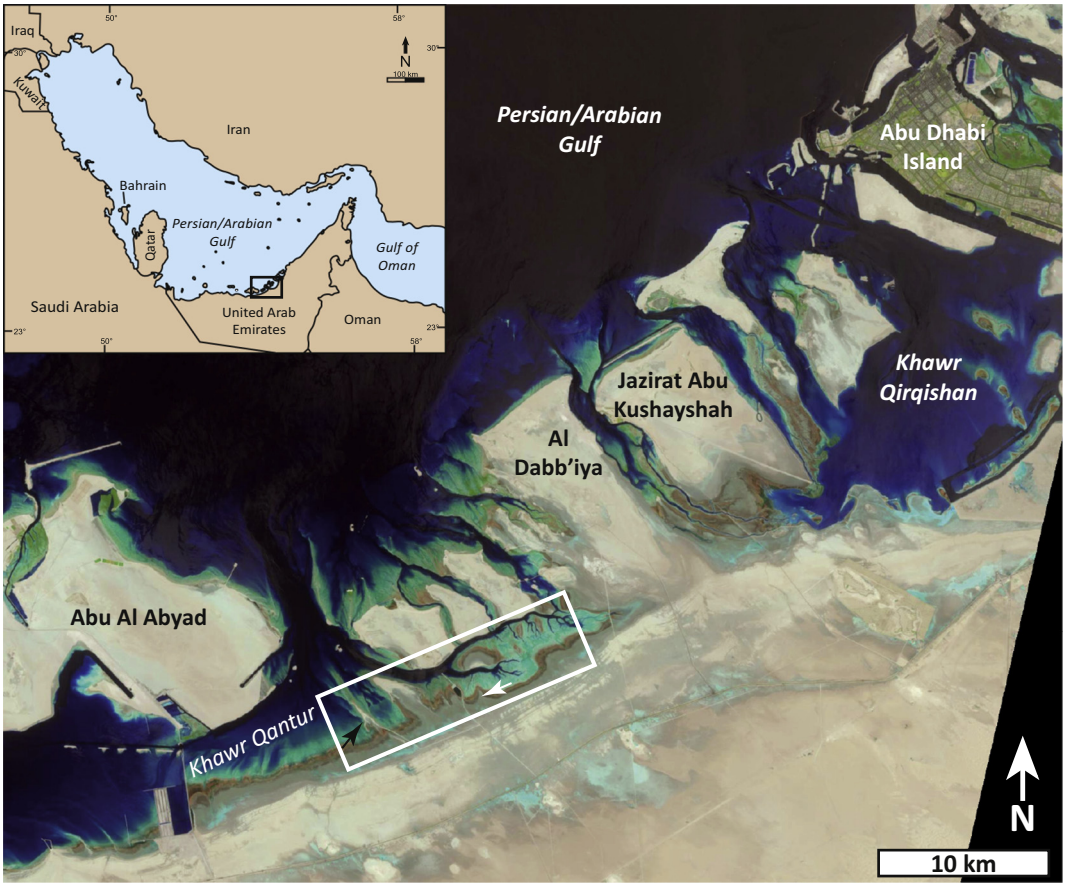

Fig. 1. Satellite image of the Abu Dhabi coastline between Abu Dhabi Island in the east and Abu al Abyad Island in the west, see inset map for regional context. The location of the 16 km-long study area is highlighted by the white box, the black arrow indicates the position of the island shown in Fig. 2, the white arrow indicates the location of Figs. 4 and 6. Landsat ETM image acquired 3rd July 2002.

invaluable resource for selecting locations for more robust, long-term monitoring. Observations were also regularly undertaken outside of the focus areas in order to ensure that the widest possible gamut of data was incorporated into the study. Field observations also included surveying two transects normal to the shoreline in order to measure the height and slope of the carbonate ramp coastal system. The survey was undertaken using an Altus APS-3 differential global positioning system (dGPS). At each measurement position, at least 10 measurements were made and the average of these was used to geolocated the position.

A particular challenge resulting from the low-angle geometry of the Abu Dhabi coastal system is demarking a definitive 'coastline'. In this carbonate ramp system the horizontal distance between mean high water and mean low water may locally exceed 4 km, with a high degree of variability resulting from even the mildest winds or atmospheric pressure variations. In the absence of a definitive coastline, we employ the microbial mat belt as a datum. The landward and seaward limits of microbial mat belts are strongly controlled by their position in the intertidal zone (Lokier and Steuber, 2008). The seaward extent of the belt is constrained by a balance between microbial mat growth rate and the presence of grazing organisms - particularly gastropods. The mat's landward limit is governed by the limits of flooding; microbial mats must be regularly inundated to avoid desiccation.

4. Evidence of shoreline change

Shorelines are highly dynamic features in a near-continuous state of morphological flux at a range of spatial and temporal scales (Woodroffe, 2008; Rankey, 2011). The dGPS survey in this study established that the upper intertidal to supratidal portion of the ramp system dips very gently seawards at an angle of between 0.07° and 0.08°. By employing the Intergovernmental Panel on Climate Change (IPCC) global mean sea level rise rate of 3.2 mm yr^{-1} for the period between 1993 and 2010 (Church et al., 2013), an average transgression rate of 2.5 ± 0.2 m yr^{-1} can be predicted. It can be anticipated that such a significant rate of transgression would result in substantial coastline change. Field and remote sensing observations of a range of erosional and constructional features from the Abu Dhabi coastline are documented herein.

A number of morphological features were monitored in the vicinity of a low-lying vegetated island in the west of the study area (Fig. 2). Unfortunately, dredging and land reclamation activity destroyed this area in 2011 thereby abruptly curtailing monitoring. Prior to this loss, a series of spits developed at the western shore of the island and migrated landwards over a monitoring period of seven years. The spits were composed of coarse sand to gravel dominated by whole and fragmented gastropods with subordinate bivalves and other skeletal allochems. These bodies migrated towards the southeast over a pustular microbial

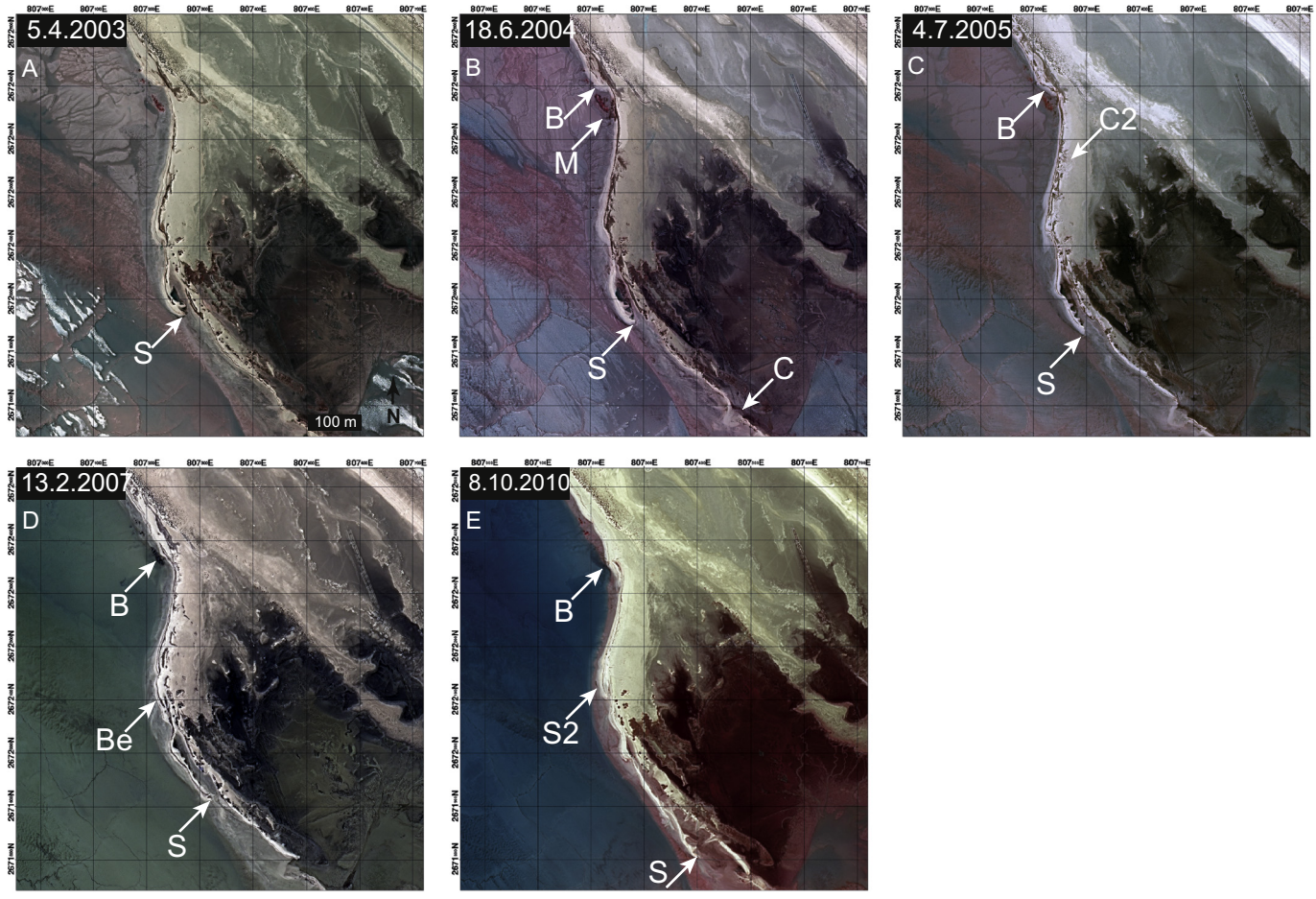

Fig. 2. Series of satellite images over a 7-year period showing geomorphological changes associated with a spit in the west of the study area (refer to Fig. 1 for the location of the images). A) Satellite image showing a series of spits landward (south) of a low-relief island. B) Spits retrograde over the microbial mat (S). In the north of the image sand bars (B) migrate south towards a stand of mangroves (M). A crevasse splay develops in the south of the image (C). C) Spits and sand bars continue to retrograde towards the south. The spit is breached with a new crevasse splay developing with an easterly orientation (C2). D) Continued southern spit migration. Sand bars begin to bury mangroves and isolate them from marine circulation. Significant building of the beach on the western margin of the spit (Be). E) Spits continue to retrograde towards the south - total migration of 218 m in 7 years and 7 months. Mangrove stand totally destroyed by migrating sand bars. New spit system developing (S2). Refer to Fig. 1 for the location within the study area. All images from Quickbird 2 (0.6 m/pixel spatial resolution for the Panchromatic Band) except those of 10/10/10 which are WorldView-2 (0.5 m/pixel resolution). Infrared is displayed as red, red as green and green as blue.

mat (Court et al., 2017) underlain by an anoxic, organic-rich mud to fine-sand grade sediment. The migration was monitored between April 2003 and August 2010 using a combination of field observations (Fig. 3A) and remote sensing imagery (Fig. 2). Over this seven and a half year period, the spit migrated 218 m landward over the microbial mats, equating to an average rate of 29 m yr^{-1}. Similar back-stepping has been observed in beach ridges elsewhere along the coast (Fig. 3B).

Storm events result in localised breaching of beach ridges to produce crevasse splays comprising coarse-grained carbonate sands (Figs. 2C, 3C). Once emplaced, these sands are not susceptible to reworking, thereby contributing to the aggradation of the island surface. Retrograding sand bodies also have a significant impact on the development of mangals (Fig. 3D–F). Where the aerial roots (pneumatophores) of mangroves are buried by migrating sands, the mangrove trees die and become vulnerable to subsequent erosion (Ellison, 1999).

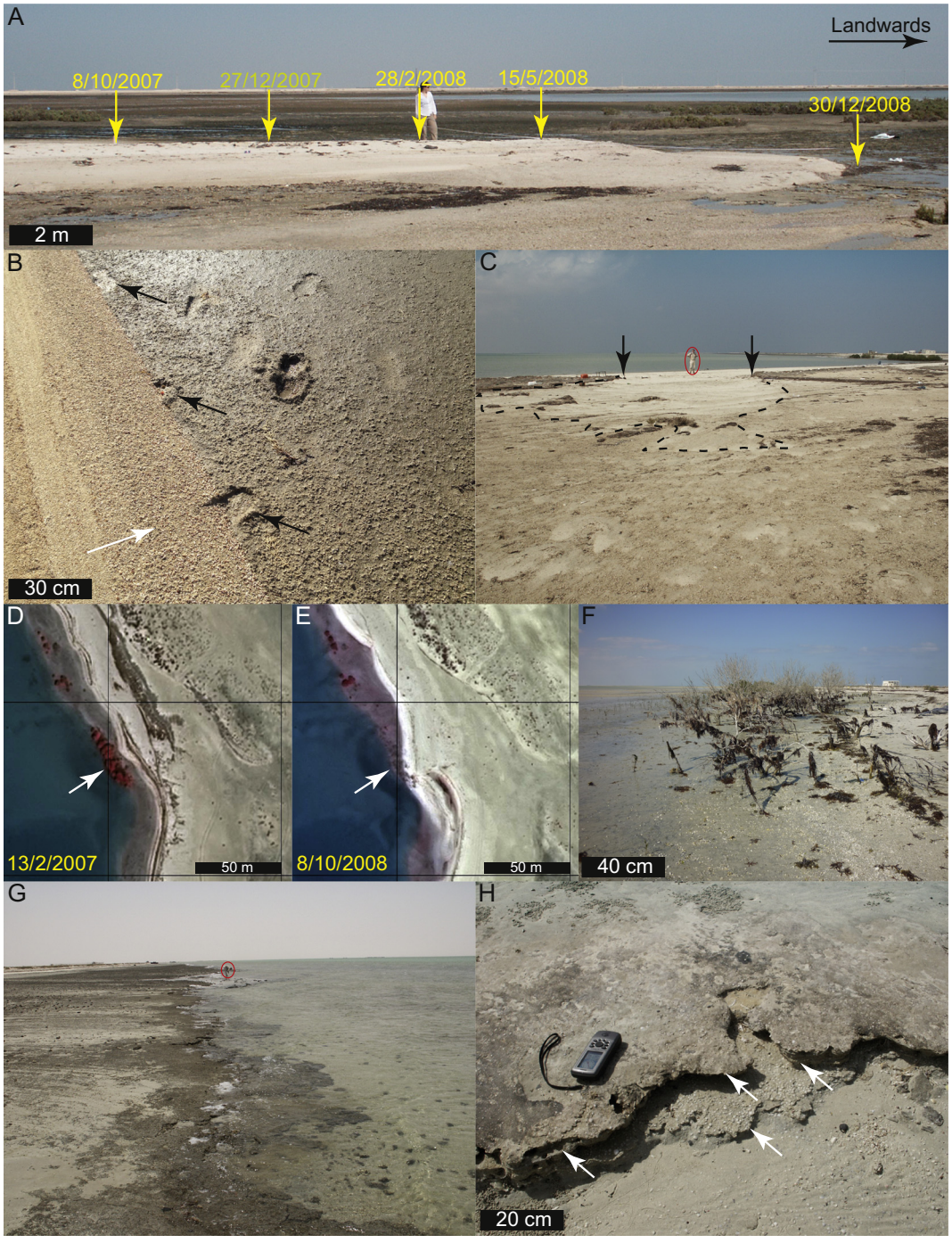

Fig. 3. Field photographs of a range of erosional and migrational features observed at the Abu Dhabi coastline. A) Observations of a spit migrating 17.5 m landwards (southeast) over the microbial mats over a period of 15 months. Arrows denote the observed location of the tip of the spit at the specified dates. B) Beach ridge back-stepping (direction of white arrow) towards the south over a microbial surface with footprints (black arrows). C) Breaching of a beach-ridge with associated crevasse splay. Black arrows indicate the limits of the breach, black dashed line denotes limit of washover (person for scale is 1.75 m tall). D & E) Paired Quickbird 2 (left) and Worldview 2 (right) satellite images showing the inundation and loss of mangroves (white arrow) by retrograding sand bodies over a period of 20 months. F) Field photograph of the mangroves killed through burial by retrograding sand bodies as indicated in panels D & E. View towards the north. G) Hardground erosion on the leeward side of the peninsula shown in Fig. 1 (bending person for scale is 1.15 m high, view towards the north). H) Erosion of microbially-bound layers of muddy sands in the upper intertidal zone, white arrows indicate distinct microbial surfaces, landwards (south) to top of image.

In the intertidal zone to the seaward and east of the island there is significant exposure and erosion of the hardgrounds (Fig. 3G). During rare higher energy storm events, clasts from the hardground are carried landward onto the surface of the sabkha where they are incorporated as a minor component into beach ridges or more muddy facies as angular extraclasts. Erosion is also observed at the landward limit of the intertidal zone. Firmgrounds, formed through the binding of sediments by interstitial microbial growth, are being eroded (Fig. 3H). Fragments of the firmground are easily abraded to form sub-rounded intraclasts or, if transported more distally, potentially extraclasts.

Within the middle to lower intertidal zone, tidal creeks are retrograding through headward erosion of the underlying hardground facies. Retrograding lobes of the intertidal bioclastic and peloidal sands locally divert the most-landward portion of the intertidal creeks; this process sometimes diverts ebb tidal flow to a different creek catchment resulting in abandonment of the old creek system (Fig. 4).

4.1. Migration of facies belts

As mentioned previously, the extent of the microbial mat belt is strongly controlled by its position within the upper part of the intertidal zone. The community composition, morphological characteristics and resilience of the microbial mats are particularly susceptible to any changes in the amount and duration of tidal flooding and any changes in energy within the depositional system.

The areal extent of the microbial mat belt can be clearly defined from satellite imagery (Fig. 4). In the field, it is possible to sub-divide the microbial mat belt into a number of morphological sub-zones (Court et al., 2017). No bioturbation is observed within the microbial mat belt or in facies landward of the microbial mats. During the period of observation, a variety of changes have been observed in relation to the microbial mat belt.

Satellite and field observations show that both the seaward and landward margins of the microbial mats are migrating landwards (Fig. 4). The seaward margin of the mats is being buried beneath the back-stepping bioclastic and peloidal sands of the intertidal zone (Fig. 5A–E). Between February 2007 and September 2010 the seaward margin of the microbial mats locally retrograded by between 60 and 100 m, equivalent to a rate of 16–27 m yr^{-1}. The retrograding bioclastic and peloidal sands initially cover the mat surface with a thin sediment veneer (Fig. 5A) that results in a morphological change in the growth of the mats. Low-lying areas of the mat and gaps between polygons (Fig. 5B) are preferentially covered by sediment thereby reducing the small-scale relief of the mat surface. Within weeks, this sediment is colonised and stabilised by interstitial microbial growth (Fig. 5C). Topographically higher areas of the microbial mats, such as mat margins continue to grow but are increasingly susceptible to grazing by benthic

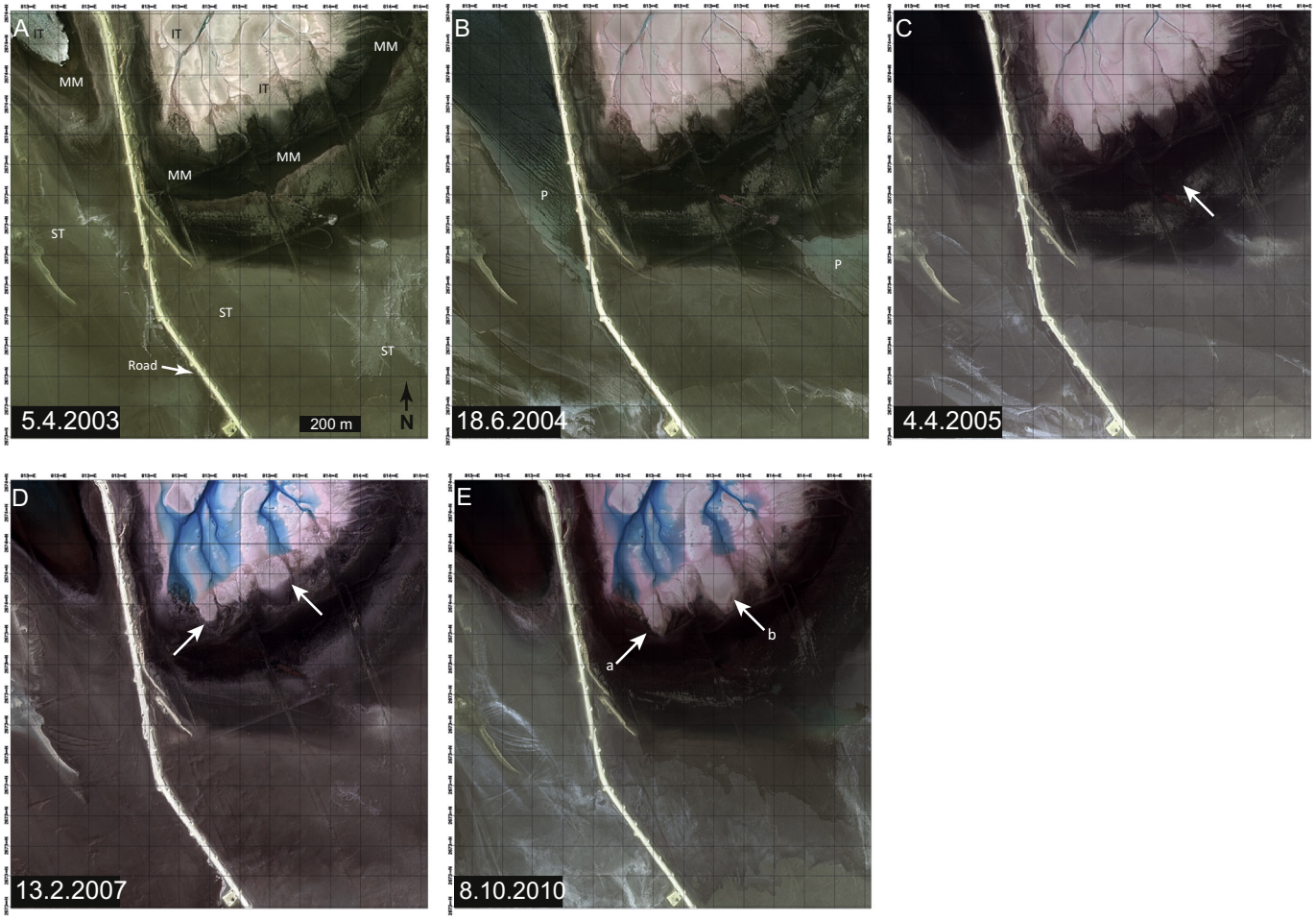

Fig. 4. Series of satellite images over a 7-year period showing geomorphological changes associated with the microbial mat belt, refer to Fig. 1 for the location of the images. A) Satellite image showing the supratidal (ST), microbial mat belt (MM) and intertidal (IT) environments of the Abu Dhabi Sabkha. B) Unusually high tides result in flooding and ponding of water in the supratidal zone (P). C) Increased microbial mat development in the north-western flooded area. Retrogradation of the landwards margin of the microbial mat belt in much of the area (arrow). D) Image with flooding of tidal creeks, intertidal bioclastic and peloidal sand facies retrograde over the microbial mat belt (arrows). E) Intertidal sands have back-stepped over a distance of 60 m at 'a' and 100 m at 'b'. The landward margin of the microbial mats has migrated landwards by only 35 m over the same period. All images from Quickbird 2 (0.6 m/pixel spatial resolution for the Panchromatic Band) except those of 8/10/10 which are WorldView-2 (0.5 m/pixel resolution). Infrared is displayed as red, red as green and green as blue.

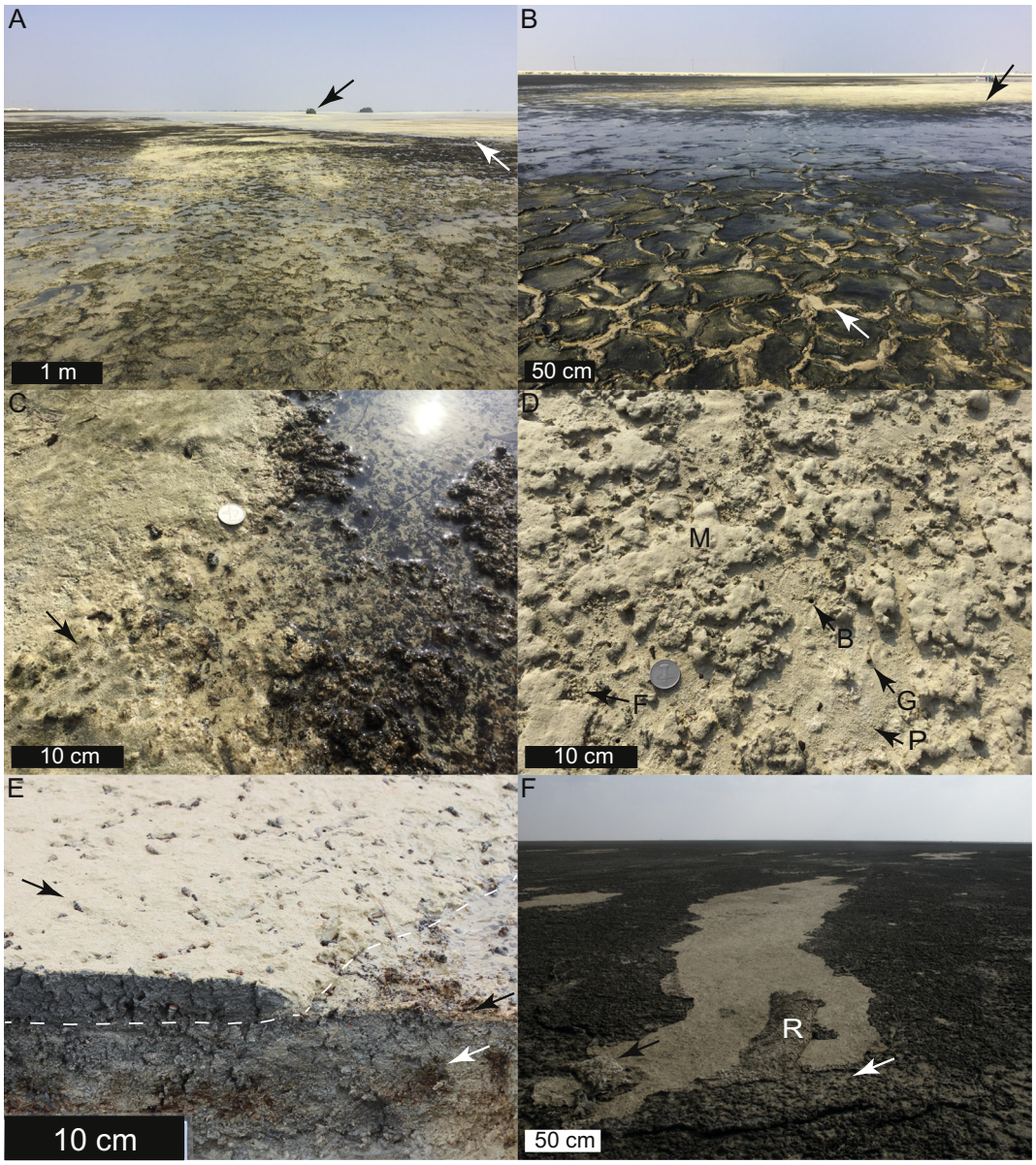

Fig. 5. Field photographs of transgressive features associated with the microbial mat belt. A) View seawards showing the backstepping of the lower intertidal bioclastic and peloidal sand facies over microbial mats with a poorly-defined polygonal morphology. The retrogradational front is indicated by the white arrow. Small stands of mangroves can be seen in the distance (black arrow). B) Well-developed leathery polygonal microbial mats (foreground) being buried by the backstepping bioclastic and peloidal sand facies (black arrow) – view towards the north (seawards). Note how the sands are infilling areas between the uplifted polygon margins (white arrow), thereby effectively 'smoothing' the topography. C) Bioclastic and peloidal sand facies (left of image, seawards) retrograding over spongy microbial mat (right of image, landwards). The sands are being stabilised by the development of a thin interstitial microbial growth within the sediment surface (black arrow). D) Following burial beneath the bioclastic and peloidal sand facies, the microbial mats (M) are susceptible to degradation. Surface feeding by gastropods (G) and crabs produces peloids (P) and feeding pellets (F) respectively. Infaunal bioturbation is limited to dwelling burrows of *Scopimera crabicauda* (B). Note that all of the burrowing and feeding is concentrated in the topographically low areas where these microbial mats are absent. E) Cross section showing the laminated bioclastic and peloidal sand facies (arrow) retrograding over the spongy microbial mat (black arrow) - the dashed white line demarks the base and front of the transgressing unit. The surface of the sands is colonised by an interstitial pale green microbial community. The dark grey colour of the underlying sediments reflects the anoxic conditions in the sub-surface where microbial mats have decayed with only isolated relics remaining (white arrow). F) Areas of ripped up pustular mat – view towards the south (landwards). Areas of mat are dislodged during inundation by higher-energy events, such as storms, or through simple floating when gas is trapped below the impermeable mat. The displaced material may be overturned (black arrow), piled up (white arrow) or form elongate roles (R).

fauna that reside within the now-adjacent sands. With increasing burial, and over time, the microbial mats become susceptible to degradation. Increased flooding of the microbial mats, and the presence of host sediment, facilitates the presence of increased numbers of grazing fauna dominated by gastropods, ostracods and crabs (Fig. 5D). The presence of a significant organic component within the sediment results in the onset of anoxic conditions immediately below the sediment surface (Fig. 5E). Burrowing is absent from the microbial mats and supratidal facies. is limited to simple shallow dwelling burrows constructed by crabs (*Scopimera crabicauda*). Burrows are absent.

The landward margin of the microbial mats is also back-stepping throughout the study area, though, at a rate of only 10 m yr^{-1} this is significantly slower than the retrogradation of the seaward margin over the same observation period (Fig. 4). The disparity in the retrogradation rates between the seaward and landward margins of the microbial mat belt has resulted in the belt becoming significantly narrower as can be clearly visualised from Normalized Difference Vegetation Index images (Fig. 6). Throughout the study area the landward margin of the microbial mat belt is characterised by a thin pustular mat that is developing above a mixed carbonate-evaporite sequence with abundant sand to

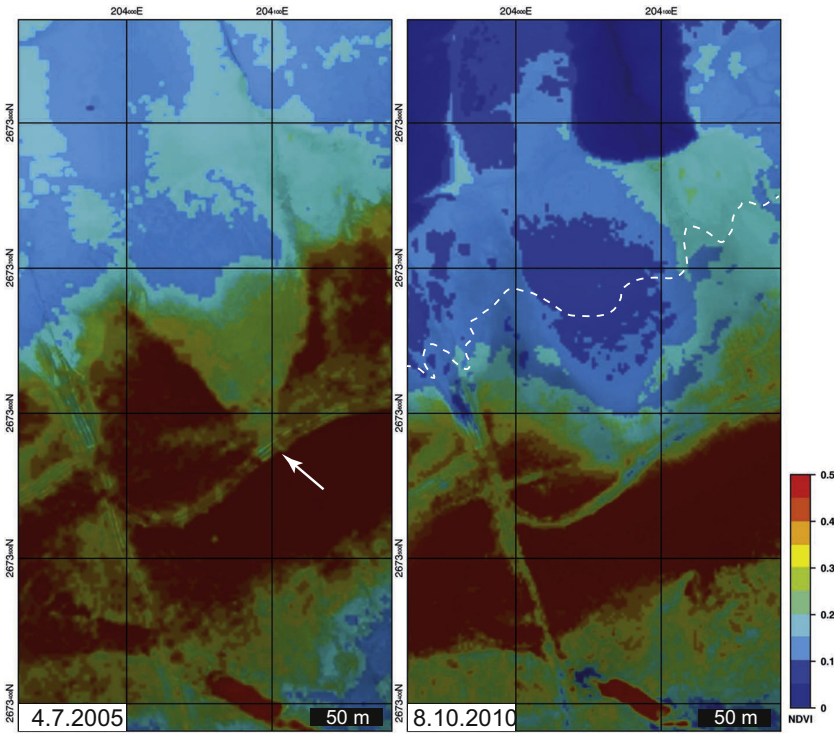

Fig. 6. Paired Normalized Difference Vegetation Index images from 4/7/2005 (Quickbird 2) and 8/10/2010 (Worldview 2) showing that the seaward limit of the microbial mat belt has moved significantly landward while the landward limit has retrograded to a lesser extent over the 5 years of observation. The dashed white line shows the former position of the seaward margin of the microbial mat. Distribution of the vegetation, including microbial mats, is highlighted by the green to red colours. The trackways seen in the images (white arrow) are a result of seismic trucks surveying the area during the 20th Century. The location of the image is indicated by the white arrow in Fig. 1.

gravel grade gypsum. The gypsum was formed through the evaporation of groundwater in the shallow sub-surface of the supratidal sabkha (Lokier and Steuber, 2008).

During fieldwork, large areas of the microbial mat were observed to episodically be removed either during rare higher-energy storm events or more gently through rafting resulting when trapped gas below the impermeable mat surface buoys-up the mat during periods of excessive flooding. Such denudation exposes the underlying sediment (Fig. 5F) either to renewed microbial colonisation or, likely in the case of storm-events, to erosion to form localised depressions that may develop into intertidal ponds (Paul et al., in prep.).

5. Discussion

The remote sensing and field observations documented in this study record a shoreline that has entered a phase of erosion and retrogradation consistent with the onset of marine transgression. This provides an exceptional opportunity to establish the diagnostic sedimentary features that would provide evidence of transgression of a carbonate ramp system within the geological record. Employing the axiom that improved knowledge of the past and present are key to more accurate predictions of the future, we conjecture the likely future effects of shoreline retreat and implications thereof.

5.1. Calculated transgression compared with measured retrogradation

Under the tectonically stable conditions of the southern Gulf shoreline (Stevens et al., 2014; Lokier et al., 2015; Pfeffer and Allemand, 2016), relative sea level can be considered as equivalent to eustatic sea level over the duration of the study. The predicted average rate of flooding for the Abu Dhabi coastline of 2.5 ± 0.2 m yr^{-1} is much lower than any of the observed rates of coastal feature retrogradation, *i.e.* 10–29 m yr^{-1}. Consequently, eustatic sea-level rise accounts for only an average of 15% (8.6–25%) of the observed shoreline retreat, a figure that is very similar to the 12% noted from the open beaches of the Mediterranean coast of France (Brunel and Sabatier, 2009). This large discrepancy arises from the assumption that marine transgression is a passive submersion process without modification of the shoreline. Such a model is over-simplified because during transgression coastal landforms are forced to migrate in order to maintain their specific position in relation to the coastal energy gradient (Pethick, 2001). It is inferred that this model of dynamic active submersion (Brunel and Sabatier, 2009) will expose the coastline to increased erosion (Leatherman et al., 2000; Woodroffe, 2008) and result in shorelines retreating at a rate greater than that predicted for sea-level rise alone. Further, the carbonate factory in these shallow to intertidal environments does not produce sufficient sediment to fill the accommodation space newly created by rising sea level; a situation that is compounded by the lack of fluvial systems and the prevailing onshore, Shamal, wind both of which prevent the influx of detrital sediment from the land.

It is widely accepted that the much-employed Brunn (1962) model for shoreline retreat is over-simplified, neglecting site-specific geomorphological and sedimentological factors (Cooper and Pilkey, 2004). The model is particularly inadequate in the vicinity of barrier islands, capes and spits (Leatherman et al., 2000). Local-scale variations in the geomorphological response of the coastline to sea-level change are common (Webb and Kench, 2010; Ford and Kench, 2015; Romine et al., 2016), with adjacent portions of the coastline variously displaying erosion, accretion or no significant change. The nature of the response is controlled by the antecedent topography (Romine et al., 2016), changes in boundary conditions (Webb and Kench, 2010) and sediment supply (Carrasco et al., 2016; Testut et al., 2016).

5.2. Recognising transgression in the stratigraphic record

Can the present-day flooding at the Abu Dhabi coastline be considered as representative of a transgressive event in the true sequence

stratigraphic context? Transgression may be defined as a landward shift of the marine system initiated where base-level rises at a rate higher than the shoreline sedimentation rate (Catuneanu et al., 2009). The transgressive part of the sequence lies immediately on the maximum regressive surface (transgressive surface) of the previous regressive phase (Catuneanu et al., 2011). Presented with these definitions, we conclude that the observations made during this study support the interpretation that the Abu Dhabi coastline has entered a phase of transgression recording the transition from a progradational to a retrogradational geometry of the sedimentary bodies.

The architecture of transgressive deposits is a product of the rate of sediment supply, the rate of sea-level change, the geomorphology of the shoreline system and the energy regime – a single transgressive transect comprises sectors recording deposition and sectors of erosion (Cattaneo and Steel, 2003). The relatively high rate of relative sea-level rise, low-angle geometry and limited sediment supply at the Abu Dhabi coastline support a non-accretionary transgressive shoreline trajectory (*sensu* Helland-Hansen and Gjelberg, 1994). Under these conditions, a rapid landward shift in the shoreline would be expected to initially produce only thin transgressive deposits with *in situ* drowning of the shoreface (Cattaneo and Steel, 2003). This is particularly the case in carbonate-dominated systems where a lag time of a few hundred to a few thousand years is common before the carbonate factory is fully functioning again (Tipper, 1997; Kemp and Sadler, 2014).

The presence of cohesive, microbially-bound, fine-grained sediment further inhibits the formation of a tidal ravinement surface, except where headward erosion occurs at the thalweg of tidal channels. Headward erosion of tidal creeks has been documented from other settings (Knighton et al., 1991; Rankey and Morgan, 2002). During high tides, seawater incursion is concentrated within slight topographic depressions, the centre of which becomes increasingly susceptible to tidal scouring and subsequent deepening (Knighton et al., 1991). This process is producing highly localised tidal ravinement surfaces where tidal creeks erode the underlying hardground.

Transgressive lags, occurring as either conglomeratic, glauconitic, fossiliferous or geochemical deposits (Kidwell, 1989; Cattaneo and Steel, 2003), are typically expected where there is sediment starvation of the shelf (Swift, 1976) or condensation resulting from dynamic bypass (Kidwell, 1989). Lag deposits are not observed in the current study as there is a paucity of bioclasts, intraclasts or extraclasts. Although eroded firmground and hardground clasts were observed, these were relatively rare and only locally concentrated in, for example, beach ridges or spits. Carbonate sedimentation rates, though low at 13–50 cm/ky (Kinsman, 1969; Lokier and Steuber, 2008), are sufficient to prevent sediment starvation.

It has previously been inferred that, within tidal flat systems, new accommodation is initially rapidly filled by microbial mats (Strasser, 2015) until they are sufficiently inundated to permit grazing organisms to destroy them (Farmer, 1992). During the present study, we observe a distinct narrowing of the microbial mat belt at the coastline. The superposition of the back-stepping upper intertidal microbial mats over supratidal-deposited evaporite facies forms a distinct stratigraphic relationship that is indicative of transgression (Lokier et al., 2013). Should the microbial mats be rapidly buried, increasing the likelihood of preservation, then they may act as an aquitard preventing dissolution of the underlying evaporite facies and allowing their retention into the burial regime. Where the surface microbial mat belt is destroyed, either during higher energy events such as storms or through the headward erosion of tidal channels, the underlying unlithified sediment is exposed and is susceptible to erosion.

Bioturbation is limited to the intertidal and subtidal facies that lie seaward of the microbial mat belt. During flooding, the surface microbial mat becomes accessible to a range of grazing and burrowing fauna (Lokier and Steuber, 2008). However, the retrograding facies rapidly bury the organic-rich microbial mats, resulting in the onset of anoxic conditions in the shallow sub-surface and a consequent inhibition of infaunal detrital sediment feeders. Burrows are limited to shallow, open, dwelling burrows and bioturbation is unlikely to be so intensive as to destroy primary sedimentary structures. Under these conditions, the onset of bioturbation locally records the onset of transgression. Locally, microbial mats are rapidly (hours to weeks) buried beneath relatively-thick coarse grained carbonate sands, associated with the retrogradation of spits or washover deposits. Under these circumstances the buried microbial mat will be isolated from bioturbation resulting in a sedimentary sequence characterised by coarse-grained sediments directly overlying finer grained facies displaying a microbial lamination and lacking faunal bioturbation.

5.3. Projections of 21st century transgression

Based on different Representative Concentration Pathways (RCP) scenarios, the IPCC 5th Assessment Report predicts a likely global mean sea-level rise of between 0.44 (0.28–0.61) m (RCP2.6) and 0.74 (0.52–0.98) m (RCP8.5) by the year 2100 (Church et al., 2013). Given that there is currently no significant vertical land motion (subsidence or tectonic uplift) at the southern shore of the Gulf (Pfeffer and Allemand, 2016), these global mean sea-level rise figures can be employed to predict the range of the degree of likely flooding of the natural Abu Dhabi coastline.

Based on the angle of slope and the amount of projected sea level rise it is calculated that by 2100 the amount of total passive flooding is to be likely between 340 (216–471) m (RCP2.6) and 571 (401–756) m (RCP8.5) (Fig. 7). The rate of flooding at the Abu Dhabi coastline is calculated to lie in the range between 3.40 (1.54–5.25) m yr^{-1} (RCP2.6) and 8.64 (5.79–12.12) m yr^{-1} (RCP8.5) by the year 2100. This would result in a significant reduction in land area in natural coastal systems.

The above figures assume passive flooding of the coastline without any dynamic response to sea-level rise, as discussed earlier. Adopting an assumption that sea-level rise will continue to account for only 15% of shoreline retreat, we can significantly revise the above figures. The amount of total dynamic flooding by 2100 would be likely between 2.26 (1.44–3.14) km (RCP2.6) and 3.81 (2.68–5.04) km (RCP8.5). Since most of the Abu Dhabi coastline is not embanked by a cliff or scarp, there is no theoretical limit to the amount of landward migration of the shoreline.

Of course, the assumption that sea-level rise will continue to contribute only 15% of shoreline regression for the remainder of the 21st century is highly conjectural and open to significant error. Localised variations in sediment availability and transport pathways make predictions highly challenging (Romine et al., 2016). The creation of new accommodation and onset of improved marine circulation may promote a positive response from the carbonate factory (Eberli, 2013), with an increase in carbonate production that may go some way to offsetting the transgressive process. Conversely, as surface water temperatures rise and pH decreases the stress on marine organisms will inhibit carbonate production. As has been documented elsewhere, there is normally a significant lag time before the organic carbonate factory is fully established (Kemp and Sadler, 2014). In the low-angle carbonate ramp setting, the transport of sediments will be controlled by waves and tides. Increased water depth will result in greater wave energy reaching the shore thereby increasing shoreline erosion (Woodroffe, 2008) and sediment reworking; likewise, tidal energy may locally increase or decrease (Cattaneo and Steel, 2003).

The sedimentary column in the shallow sub-surface of the Abu Dhabi coastline contains a significant proportion of evaporite minerals (Lokier and Steuber, 2008) that will be highly susceptible to *in situ* dissolution during marine flooding. Where these sediments are mechanically eroded, their dissolution will be even more rapid and they will not contribute to the sediment supply. The loss of these evaporite minerals will further limit the supply of reworked sediment during the flooding phase.

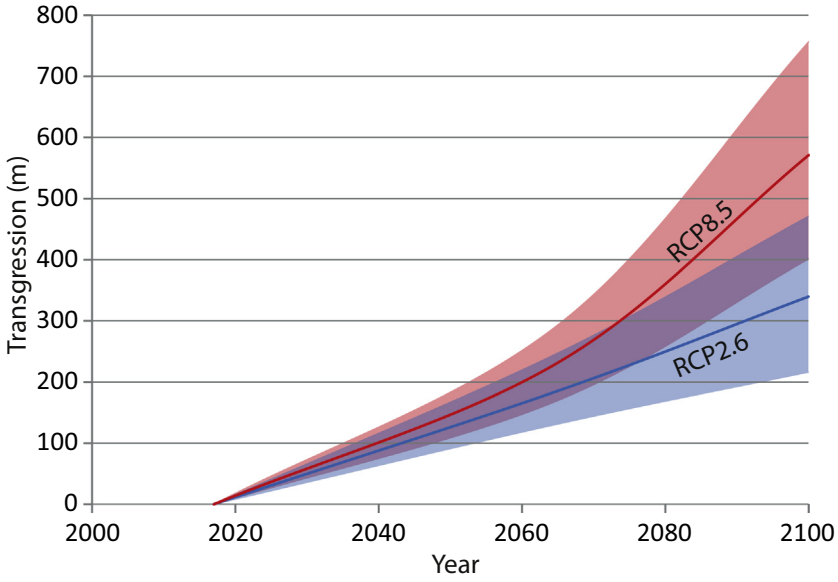

Fig. 7. Calculated ranges of transgression of the natural Abu Dhabi coastline for the 21st century for IPCC RCP2.6 and RCP8.5 scenarios.

5.4. Environmental and societal implications

The calculated figures for transgression of the Abu Dhabi coastline, even those assuming passive flooding, have significant environmental and societal implications. Natural ecosystems are unlikely to respond positively to such rapid inundation, it is likely that mangals and microbial mats will be most affected. Increasing energy at the shoreline will further erode microbial mats while increased inundation will inhibit recolonisation. Flooding will drown mangroves, with sediment smothering of their aerial pneumatophores resulting in the death of the trees (Ellison, 1999) and the loss of mangals. The loss of the mangal and microbial mat communities will have significant impacts on the protection and stabilisation of coastal sediments, enhancing erosion and further promoting shoreline retreat.

The societal implications of sea-level rise are enormous. Globally, in excess of 2 billion people (37% of global population) live within 100 km of a coastline (Cohen et al., 1997) with over 145 million people living within 1 m of present day mean sea level (Anthoff et al., 2006). In the United Arab Emirates *c.* 5 million people (85.5% of the population) reside in the low-lying cities of the Gulf coastline (DESA, 2016). Management of the coastal system requires predictive rates of transgression and geomorphic change (Pethick, 2001; Brunel and Sabatier, 2009). More accurate predictions can be achieved through the establishment of a continuous, long-term, high-frequency, monitoring program recording *in situ* oceanic and meteorological parameters in tandem with satellite observations and regular geodesic surveys of coastline transects. These observations should be supported by surveys of coastal sedimentary facies geometries and sediment transport pathways in order to understand the role of sediment supply and loss within the coastal system.

6. Conclusions

Numerous lines of sedimentological and geomorphological observations have been employed to conclude that the present-day Abu Dhabi coastline has entered a period of marine transgression. Measured rates of retrogradation (10–29 m yr^{-1}) are significantly higher than the likely rate of flooding calculated from IPCC predicted sea-level rise alone (2.5 ± 2 m yr^{-1}). This discrepancy is reconciled by the application of an inferred dynamic flooding scenario in which rising sea-level increases the energy regime at the shoreline, thereby facilitating erosion and enhancing shoreline retreat. The low-angle carbonate ramp setting supports a non-accretionary transgressive shoreline trajectory with little likelihood of a well-developed ravinement surface or of transgressive lag deposits. The onset of transgression in such a context may be difficult to recognise in the stratigraphic record. Identification would be aided by the recognition of back-stepping of marine facies, the burial of microbial mats and the onset of bioturbation by marine organisms.

Employing IPCC RCP scenarios for future sea-level rise and the angle of slope of the coastal system, calculated likely total passive flooding of the Abu Dhabi coastline ranges between 340 m and 571 m by the year 2100, at a rate of between 3.40 m yr^{-1} and 8.64 m yr^{-1}. These values increase significantly if it is assumed that future flooding will continue to be dynamic, at a rate akin to that observed during the duration of the current study. Under this scenario, calculated likely total dynamic flooding by 2100 would be between 2.26 km and 3.81 km. All of these figures, both passive and dynamic, imply a significant reduction in land area with substantial environmental and societal consequences.

Acknowledgments

The authors are grateful to Japan Oil Development Company Ltd. (JODCO) and JGI Inc. for sponsoring the processing of the satellite images utilised in this paper. We thank André Strasser and an anonymous reviewer for their insightful and constructive comments. We also acknowledge Editor Andrew James Plater for his guidance through the editorial process.

References

Anthoff, D., Nicholls, R.J., Tol, R.S., Vafeidis, A.T., 2006. Global and Regional Exposure to Large Rises in Sea-level: A Sensitivity Analysis. Tyndall Centre for Climate Change Research, p. 96 working paper.

Bottomley, N., 1996. Recent climate of Abu Dhabi. In: Osborne, P.E. (Ed.), Desert Ecology of Abu Dhabi. A Review and Recent Studies. Pisces, Newbury, pp. 36–49.

Brunel, C., Sabatier, F., 2009. Potential influence of sea-level rise in controlling shoreline position on the French Mediterranean Coast. Geomorphology 107 (1–2), 47–57.

Brunn, P., 1962. Sea-level rise as a cause of shore erosion. Proceedings of the American Society of Civil Engineers. Journal of the Waterways and Harbour Division vol. 88, pp. 117–130.

Carrasco, A.R., Ferreira, Ó., Roelvink, D., 2016. Coastal lagoons and rising sea level: a review. Earth Sci. Rev. 154, 356–368.

Cattaneo, A., Steel, R.J., 2003. Transgressive deposits: a review of their variability. Earth Sci. Rev. 62 (3–4), 187–228.

Catuneanu, O., Abreu, V., Bhattacharya, J.P., Blum, M.D., Dalrymple, R.W., Eriksson, P.G., Fielding, C.R., Fisher, W.L., Galloway, W.E., Gibling, M.R., Giles, K.A., Holbrook, J.M.,

Jordan, R., Kendall, C.G.S.C., Macurda, B., Martinsen, O.J., Miall, A.D., Neal, J.E., Nummedal, D., Pomar, L., Posamentier, H.W., Pratt, B.R., Sarg, J.F., Shanley, K.W., Steel, R.J., Strasser, A., Tucker, M.E., Winker, C., 2009. Towards the standardization of sequence stratigraphy. Earth Sci. Rev. 92 (1–2), 1–33.
Catuneanu, O., Galloway, W.E., Kendall, C.G.S.t.C., Miall, A.D., Posamentier, H.W., Strasser, A., Tucker, M.E., 2011. Sequence stratigraphy: methodology and nomenclature. Newsl. Stratigr. 44 (3), 173–245.
Church, J.A., White, N.J., 2011. Sea-level rise from the late 19th to the early 21st century. Surv. Geophys. 32 (4), 585–602.
Church, J.A., Clark, P.U., Cazenave, A., Gregory, J.M., Jevrejeva, S., Levermann, A., Merrifield, M.A., Milne, G.A., Nerem, R.S., Nunn, P.D., Payne, A.J., Pfeffer, W.T., Stammer, D., Unnikrishnan, A.S., 2013. Sea level change. In: Stocker, T.F., Qin, D., Plattner, G.-K., Tignor, M., Allen, S.K., Boschung, J., Nauels, A., Xia, Y., Bex, V., Midgley, P.M. (Eds.), Climate Change 2013: The Physical Science Basis: Working Group I Contribution to the Fifth Assessment Report of the Intergovernmental Panel on Climate Change. Cambridge University Press, Cambridge, United Kingdom and New York, NY, USA, pp. 1137–1216.
Cohen, J.E., Small, C., Mellinger, A., Gallup, J., Sachs, J., 1997. Estimates of coastal populations. Science 278 (5341), 1209–1213.
Cooper, J.A.G., Pilkey, O.H., 2004. Sea-level rise and shoreline retreat: time to abandon the Bruun rule. Glob. Planet. Chang. 43 (3–4), 157–171.
Court, W.M., Paul, A., Lokier, S.W., 2017. The preservation potential of environmentally diagnostic sedimentary structures from a coastal sabkha. Mar. Geol. 386, 1–8.
DESA, 2016. World Statistics Pocketbook 2016. 2016. United Nations, New Yourk, USA.
Eberli, G.P., 2013. The uncertainties involved in extracting amplitude and frequency of orbitally driven sea-level fluctuations from shallow-water carbonate cycles. Sedimentology 60 (1), 64–84.
Ellison, J.C., 1999. Impacts of sediment burial on mangroves. Mar. Pollut. Bull. 37 (8–12), 420–426.
Emery, K.O., 1956. Sediments and water of Persian Gulf. AAPG Bull. 40 (10), 2354–2383.
Evans, G., 1966. The recent sedimentary facies of the Persian Gulf region. Philos. Trans. R. Soc. 259, 291–298.
Evans, G., Kirkham, A., 2002. Distribution of sabkhat within the Arabian Peninsula and the adjacent countries. In: Barth, H.J., Böer, B. (Eds.), Sabkha Ecosystems Volume 1: The Arabian Peninsula and Adjacent Countries. Tasks for Vegetation Science. Springer, Netherlands, pp. 7–20.
Evans, G., Kinsman, D.J.J., Shearman, D.J., 1964. A reconnaissance survey of the environment of recent carbonate sedimentation along the Trucial Coast, Persian Gulf. In: Van Straaten, L.M.J.U. (Ed.), Deltaic and Shallow Marine Deposits: Proceedings of the 6th International Sedimentological Congress The Netherlands and Belgium - 1963. Developments in Sedimentology. Elsevier, Amsterdam, pp. 129–135.
Evans, G., Schmidt, V., Bush, P., Nelson, H., 1969. Stratigraphy and geologic history of the sabkha, Abu Dhabi, Persian Gulf. Sedimentology 12, 145–159.
Farmer, J., 1992. Grazing and bioturbation in modern microbial mats. In: Schopf, J.W.a.K. (Ed.), The Proterozoic Biosphere. Cambridge University Press, New York, pp. 295–297.
Ford, M.R., Kench, P.S., 2015. Multi-decadal shoreline changes in response to sea level rise in the Marshall Islands. Anthropocene 11, 14–24.
Harris, P.M., 1994. Satellite images and description of study area. In: Harris, P.M., Kowalik, W.S. (Eds.), Satellite Images of Carbonate Depositional Settings. Methods in Exploration Series. American Association of Petroleum Geologists, pp. 29–139.
Helland-Hansen, W., Gjelberg, J.G., 1994. Conceptual basis and variability in sequence stratigraphy: a different perspective. Sediment. Geol. 92 (1), 31–52.
Kemp, D.B., Sadler, P.M., 2014. Climatic and eustatic signals in a global compilation of shallow marine carbonate accumulation rates. Sedimentology 61 (5), 1286–1297.
Kidwell, S.M., 1989. Stratigraphic condensation of marine transgressive records: origin of major shell deposits in the Miocene of Maryland. J. Geol. 97 (1), 1–24.
Kinsman, D.J.J., 1969. Modes of formation, sedimentary associations, and diagnostic features of shallow-water and supratidal evaporites. AAPG Bull. 53 (4), 830–840.
Kinsman, D.J.J., Park, R.K., 1976. Algal belt and coastal sabkha evolution, Trucial Coast, Persian Gulf. In: Walter, M.H. (Ed.), Stromatolites. Developments in Sedimentology. Elsevier, pp. 421–433.
Knighton, A.D., Mills, K., Woodroffe, C.D., 1991. Tidal-creek extension and saltwater intrusion in northern Australia. Geology 19 (8), 831–834.
Leatherman, S.P., Zhang, K., Douglas, B.C., 2000. Sea level rise shown to drive coastal erosion. EOS Trans. Am. Geophys. Union Vol. 81 (6), 55–57.
Lokier, S.W., Fiorini, F., 2016. Temporal evolution of a carbonate coastal system, Abu Dhabi, United Arab Emirates. Mar. Geol. 381, 102–113.
Lokier, S., Steuber, T., 2008. Quantification of carbonate-ramp sedimentation and progradation rates for the late Holocene Abu Dhabi shoreline. J. Sediment. Res. 78 (7–8), 423–431.
Lokier, S.W., Knaf, A., Kimiagar, S., 2013. A quantitative analysis of recent arid coastal sedimentary facies from the Arabian Gulf Coastline of Abu Dhabi, United Arab Emirates. Mar. Geol. 346 (0), 141–152.
Lokier, S.W., Bateman, M.D., Larkin, N.R., Rye, P., Stewart, J.R., 2015. Late Quaternary sea-level changes of the Persian Gulf. Quat. Res. 84 (1), 69–81.
Meyssignac, B., Cazenave, A., 2012. Sea level: a review of present-day and recent-past changes and variability. J. Geodyn. 58, 96–109.
Pethick, J., 2001. Coastal management and sea-level rise. Catena 42 (2–4), 307–322.
Pfeffer, J., Allemand, P., 2016. The key role of vertical land motions in coastal sea level variations: a global synthesis of multisatellite altimetry, tide gauge data and GPS measurements. Earth Planet. Sci. Lett. 439, 39–47.
Purser, B.H., Evans, G., 1973. Regional sedimentation along the Trucial Coast, SE Persian Gulf. In: Purser, B.H. (Ed.), The Persian Gulf - Holocene Carbonate Sedimentation and Diagenesis in a Shallow Epicontinental Sea. Springer-Verlag, Berlin, pp. 211–231.
Raafat, H., 2007. Climate. In: Kumar, A. (Ed.), Physical Geography Sector Paper. Environment Agency Abu Dhabi, pp. 72–89.
Rankey, E.C., 2011. Nature and stability of atoll island shorelines: Gilbert Island chain, Kiribati, equatorial Pacific. Sedimentology 58 (7), 1831–1859.
Rankey, E.C., Morgan, J., 2002. Quantified rates of geomorphic change on a modern carbonate tidal flat, Bahamas. Geology 30 (7), 583–586.
Romine, B.M., Fletcher, C.H., Frazer, L.N., Anderson, T.R., 2016. Beach erosion under rising sea-level modulated by coastal geomorphology and sediment availability on carbonate reef-fringed island coasts. Sedimentology 63 (5), 1321–1332.
Shinn, E.A., 1969. Submarine lithification of Holocene carbonate sediments in the Persian Gulf. Sedimentology 12, 109–144.
Singh, B., 1997. Climate-related global changes in the southern Caribbean: Trinidad and Tobago. Glob. Planet. Chang. 15 (3), 93–111.
Stevens, T., Jestico, M.J., Evans, G., Kirkham, A., 2014. Eustatic control of late Quaternary sea-level change in the Arabian/Persian Gulf. Quat. Res. 82 (1), 175–184.
Stewart, J.R., Aspinall, S., Beech, M., Fenberg, P., Hellyer, P., Larkin, N., Lokier, S.W., Marx, F.G., Meyer, M., Miller, R., Rainbow, P.S., Taylor, J.D., Whittaker, J.E., Al-Mehsin, K., Strohmenger, C.J., 2011. Biotically constrained palaeoenvironmental conditions of a mid-Holocene intertidal lagoon on the southern shore of the Arabian Gulf: evidence associated with a whale skeleton at Musaffah, Abu Dhabi, UAE. Quat. Sci. Rev. 30 (25–26), 3675–3690.
Strasser, A., 2015. Hiatuses and condensation: an estimation of time lost on a shallow carbonate platform. Deposit. Rec. 1 (2), 91–117.
Swift, D.J.P., 1976. Continental shelf sedimentation. In: Stanley, D.J., Swift, D.J.P. (Eds.), Marine Sediment Transport and Environmental Management. Wiley, New York, pp. 311–350.
Testut, L., Duvat, V., Ballu, V., Fernandes, R.M.S., Pouget, F., Salmon, C., Dyment, J., 2016. Shoreline changes in a rising sea level context: the example of Grande Glorieuse, Scattered Islands, Western Indian Ocean. Acta Oecol. 72, 110–119.
Tipper, J.C., 1997. Modeling carbonate platform sedimentation—lag comes naturally. Geology 25 (6), 495–498.
Uchupi, E., Swift, S.A., Ross, D.A., 1996. Gas venting and late Quaternary sedimentation in the Persian (Arabian) Gulf. Mar. Geol. 129, 237–269.
Webb, A.P., Kench, P.S., 2010. The dynamic response of reef islands to sea-level rise: evidence from multi-decadal analysis of island change in the Central Pacific. Glob. Planet. Chang. 72 (3), 234–246.
Woodroffe, C.D., 2008. Reef-island topography and the vulnerability of atolls to sea-level rise. Glob. Planet. Chang. 62 (1–2), 77–96.